PROCEEDINGS OF SCIENCE

Measurements of inclusive WW and WZ production with ATLAS

P. Calfayan*, **on behalf of the ATLAS Collaboration**
Indiana University, USA
E-mail: philippe.calfayan@cern.ch

Measurements of the production of the electroweak bosons pairs WW and WZ have been performed in proton-proton collisions at $\sqrt{s} = 13$ TeV, using $36.1\,\text{fb}^{-1}$ of data collected by the ATLAS experiment at the Large Hadron Collider. Detector-level distributions and unfolded differential cross sections have been measured and compared to theoretical predictions at high order in perturbative QCD (up to next-to-next-to-leading order). The results of the WW analysis were interpreted in terms of an Effective Field Theory to constrain anomalous triple gauge couplings, while those from the WZ analysis enabled the determination of the W and Z polarizations for the first time from diboson events in hadronic collisions.

European Physical Society Conference on High Energy Physics - EPS-HEP2019 -
10-17 July, 2019
Ghent, Belgium

*Speaker.

PoS(EPS-HEP2019)663

1. Introduction

The productions of the electroweak (EW) boson pairs WW and WZ constitute a stringent test of the electroweak sector of the Standard Model (SM), and allows new physics at the TeV scale to be probed in a model independent way. These processes are also important backgrounds to searches for new physics, and to the Higgs boson (H) decay into WW pairs.

More specifically, the s-channel production mode of WW pairs, which involves the exchange of an off-shell EW boson, is sensitive to the WWZ and $WW\gamma$ triple gauge boson couplings, while the angular distributions of the decay products of WZ pairs allow a measurement of the W and Z polarizations.

The measurements of the production cross sections of WW [1] and WZ [2] pairs were carried out by the ATLAS experiment [3] at the LHC, considering signal enriched fiducial regions (SR). Unfolded differential cross sections were also measured and confronted with the expectation from the SM.

2. Measurement of WW production

The production cross section of WW pairs has been measured using $36.1\,\text{fb}^{-1}$ of data at $\sqrt{s} = 13$ TeV, considering both W bosons to decay leptonically, and leading to a final state including an opposite sign electron-muon pair ($e^{\pm}\mu^{\mp}$).

The signal region (SR) consists of events with exactly one pair of isolated central leptons. A veto on additional leptons is introduced to suppress the background from other multiboson processes, while the contribution from the top production is reduced by vetoing on events with central b-jets or jets having a transverse momentum (p_{T}) larger than 35 GeV. Furthermore, the Drell-Yan background is cut down by requiring the missing p_{T} in the tracker to exceed 20 GeV, and the p_{T} of the $e\mu$ system to be greater than 30 GeV. In order for the selection to be orthogonal to that of the $H \to WW$ analysis [4], events with an invariant mass of the $e\mu$ system larger than 55 GeV are excluded.

In the SR, the main background from the SM is the $t\bar{t}$ and Wt production, which contribute nearly 26% of the events observed in the region. It is determined from a top-enriched control region in data which omits the jet veto, and which is transferred to the SR via the application of an estimated jet veto efficiency. Figure 1 shows the p_{T} of the $e\mu$ system in data together with the contributions of the WW signal and the various backgrounds from the SM.

The measured fiducial production cross section of WW pairs is $379 \pm 28\,\text{fb}$, which is found to be in agreement with predictions from MATRIX [5] that are next-to-next-to-leading order (NNLO) in QCD (up to NLO for gg initial states) and include up to NLO EW corrections, as summarized in Figure 2. Moreover, additional production cross sections have been derived for different lower thresholds on the p_{T} of the jet-veto, as can be seen in Figure 3.

The total relative systematic uncertainty on the computed WW cross section is 6.7%, excluding that on the luminosity (2.1%), and mainly originates from the jet calibration, b-tagging, and modelling of the main backgrounds.

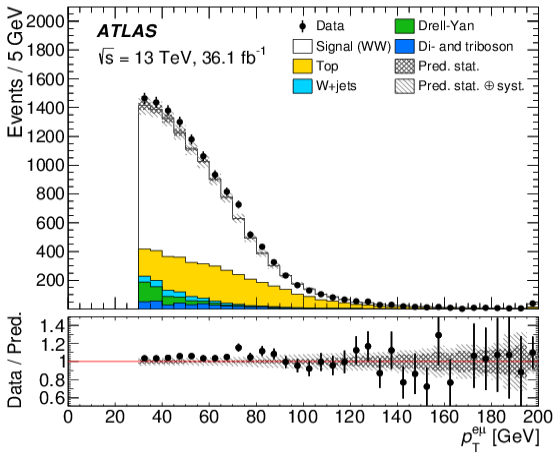

Figure 1: *WW* measurement [1]. Distribution of the transverse momentum of the $e\mu$ system in the signal region. Data (black dots) are compared to the expectation from the SM (colored histograms).

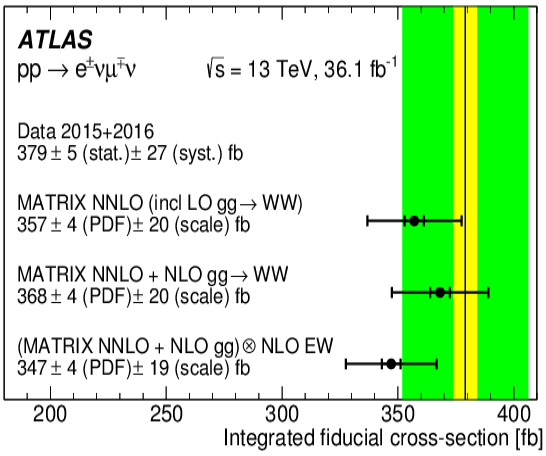

Figure 2: *WW* measurement [1]. Measured fiducial cross sections for *WW* production compared to predictions from MATRIX.

3. Measurement of WZ production

The measurement of the WZ production cross section relies on $36.1\,\text{fb}^{-1}$ of data at $\sqrt{s} = 13$ TeV, and is achieved by combining the eee, $e\mu\mu$, $ee\mu$, and $\mu\mu\mu$ channels.

The selection of candidate events in the SR requires the three leptons to be isolated, and reduces the ZZ background by vetoing on events with a least 4 looser leptons. The events are further required to include a Z boson, which is identified by selecting a pair of same-flavor and opposite sign leptons with an invariant mass compatible with that of the Z. Moreover, a W selection is performed together with a fake lepton suppression by requiring the remaining third lepton to pass tighter quality criteria, and to be compatible with a transverse mass of the W larger than 30 GeV. Figure 4 displays the transverse mass of the WZ system in data together with the contributions of the WZ signal and the various backgrounds from the SM.

The main background originates from the ZZ and $t\bar{t}+V$ production ($V \in \{W,Z\}$), which amounts to approximately 11% of events in the SR, and is determined via simulated events normalized to data from 4-leptons and 2-b-jets control regions. Events with mis-identified leptons, which constitute nearly 7% of the SR, are estimated using a fake rate from data.

The production cross section of WZ pairs, measured in the SR for the combination of all channels, equals $63.7 \pm 4.5\,\text{fb}$ and agrees with the predictions from MATRIX and SHERPA v2.2.2 [6], as highlighted in Figure 5. Furthermore, the ratio of the production cross sections of W^+Z over W^-Z events has also been computed, and is shown in Figure 6.

The fiducial WZ production cross section is measured with a total relative systematic uncertainty of 3.6%, excluding that on the luminosity, which is mostly due to the background modelling, the lepton calibration, and the pile-up.

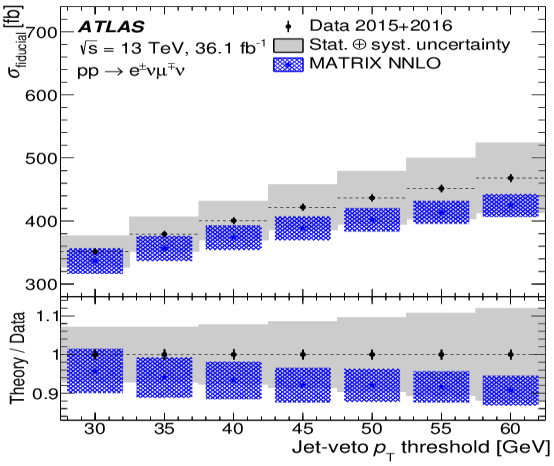

Figure 3: *WW* measurement [1]. The fiducial *WW* production cross section as a function of the lower threshold on the p_{T} of the jet-veto. Results are compared to the expectation from the SM.

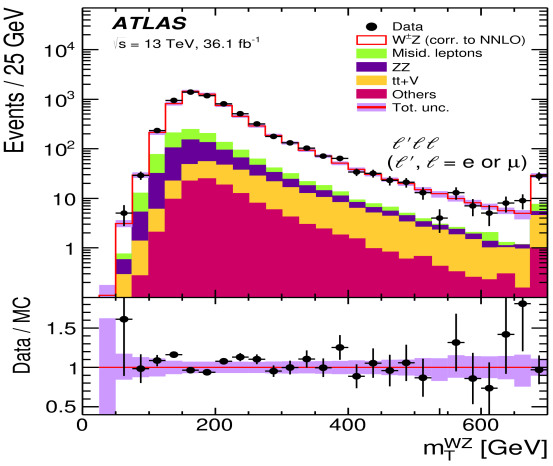

Figure 4: *WZ* measurement [2]. Distribution of the transverse mass of the *WZ* system in the signal region. Data (black dots) are compared to the expectation from the SM (colored histograms).

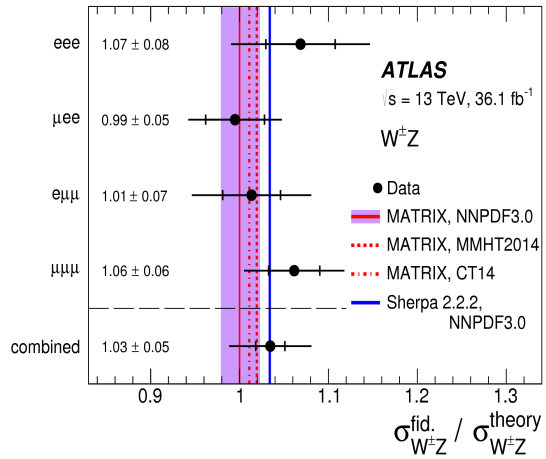

Figure 5: *WZ* measurement [2]. Measured fiducial cross sections for *WZ* production compared to the expectation from the SM. Results are provided in all the channels as well as for their combination.

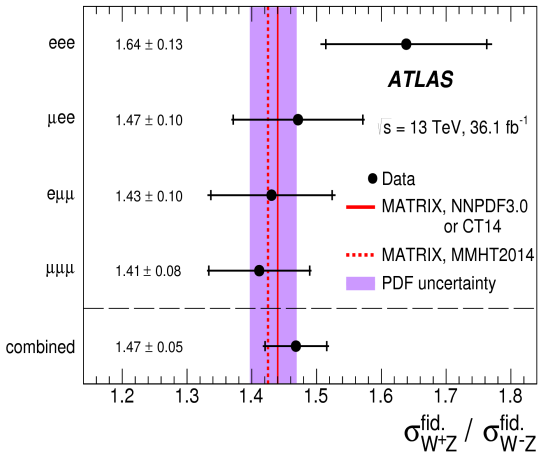

Figure 6: *WZ* measurement [2]. Ratio of the production cross sections for W^+Z over W^-Z events compared to the prediction from the SM. Results are provided in all the channels as well as for their combination.

4. Differential unfolded production cross sections

Unfolded differential cross sections have been determined via a Bayesian iterative technique [7] for the production of *WW* and *WZ* pairs in the SR, using 1 to 2 iterations and 2 to 4 iterations, respectively

The unfolded distributions are compared to an NNLO calculation of the hard matrix elements (MATRIX), and also to NLO predictions interfaced with a parton shower (POWHEG+PYTHIA8 [8,

9], POWHEG+HERWIG++ [10], and SHERPA v2.2.2).

In the WW analysis, 6 observables were considered for the unfolded distributions. Among them, the invariant mass and p_{T} of the $e\mu$ system as well as the p_{T} of the leading lepton ($p_{\mathrm{T}}^{\mathrm{lead}\,\ell}$), shown in Figure 7, characterize the energy of the production process. The other observables, namely the rapidity of the $e\mu$ system, the azimuthal angle difference between e and μ, and $\cos\theta^* = \tanh(\frac{\Delta\eta_{e\mu}}{2})$ allow the angular correlations and the spin state of the WW system to be probed.

In the WZ analysis, 8 observables were scrutinized, including the jet multiplicity, the dijet invariant mass, the p_{T} of the W and of the neutrino, and the absolute difference in rapidities between the Z and the lepton from the W decay. Furthermore, unfolded distributions of the p_{T} of the Z and of the transverse mass of the WZ system were computed, as they reveal high energy tails that are sensitive to anomalous triple gauge couplings (aTGC). The azimuthal angle difference between the W and Z bosons, which is sensitive to higher-order perturbative effects in QCD, was also unfolded and is depicted in Figure 8.

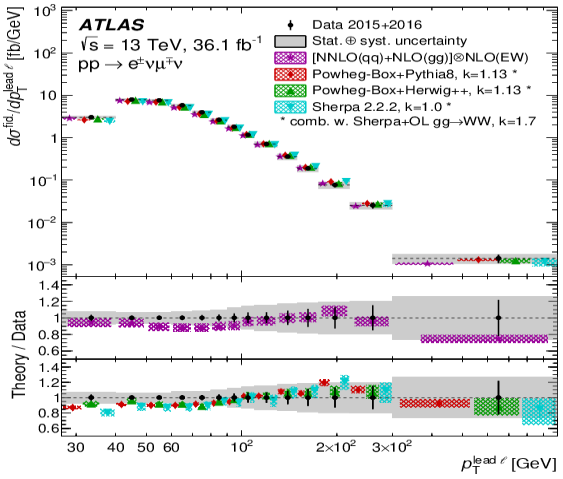

Figure 7: WW measurement [1]. Unfolded cross section for WW production in SR as a function of the p_{T} of the leading lepton. Results are compared to predictions from the SM.

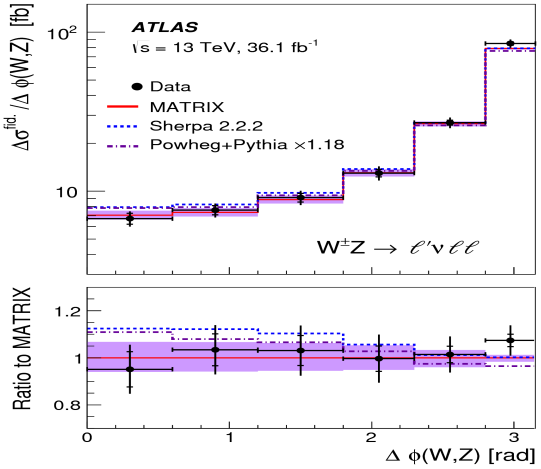

Figure 8: WZ measurement [2]. Unfolded cross section for WZ production in SR as a function of the absolute azimuthal angle difference between the W and Z bosons. Results are compared to predictions from the SM.

5. Constraints on anomalous couplings

New physics with aTGC at high energy scales (Λ) have been probed via the WWZ and $WW\gamma$ vertices associated with the WW production. The study has been achieved in the context of an Effective Field Theory with five dimension-6 operators [11] associated to the couplings c_{WWW}, c_W, c_B, $c_{\tilde{W}WW}$, and $c_{\tilde{W}}$. The signal including the aTGC was generated with MADGRAPH5_aMC@NLO [12] and interfaced with PYTHIA8.

The unfolded $p_{\mathrm{T}}^{\mathrm{lead}\,\ell}$ distribution, which highlights the high momentum transfer regime (especially in its last bin), is sensitive to the aTGC and was therefore used to constrain its strength. 95% confidence level intervals for the aTGC have thus been derived, using a profile likelihood ratio. The results, provided in Table 1, benefit from a high center-of-mass energy.

Parameter	Observed 95% CL [TeV^{-2}]	Expected 95% CL [TeV^{-2}]
c_{WWW}/Λ^2	[−3.4 , 3.3]	[−3.0 , 3.0]
c_W/Λ^2	[−7.4 , 4.1]	[−6.4 , 5.1]
c_B/Λ^2	[−21 , 18]	[−18 , 17]
$c_{\tilde{W}WW}/\Lambda^2$	[−1.6 , 1.6]	[−1.5 , 1.5]
$c_{\tilde{W}}/\Lambda^2$	[−76 , 76]	[−91 , 91]

Table 1: *WW* measurement [1]. Observed and expected 95% confidence level intervals of aTGC in the framework of a dimension-six Effective Field Theory [11].

6. Measurement of the W and Z polarisations

The W and Z polarizations have been estimated from the angular distributions of their decay products. The production cross section of WZ pairs can indeed be expressed as a function of $\cos\theta_{\ell,V}$, $\sin\theta_{\ell,V}$, and the longitudinal (f_0), left (f_L) and right-handed (f_R) helicity fractions.

The observables f_0 and f_L-f_R were determined in the fiducial region separately for W and Z in W^+Z, W^-Z, and $W^\pm Z$ events, using a profile likelihood fit of simulated templates to the observed $q_\ell.\cos\theta_{\ell,W}$ and $\cos\theta_{\ell,Z}$ (with q_ℓ being the charge of the lepton). The templates were simulated by POWHEG+PYTHIA8, and the results further corrected to particle-level.

In the case of the $W^\pm$ and Z polarizations in $W^\pm Z$ events, the measured helicity fractions (f_0 and f_L-f_R) agree within 1 to 2σ with the QCD predictions at NLO and NNLO, as illustrated in Figure 9 and 10.

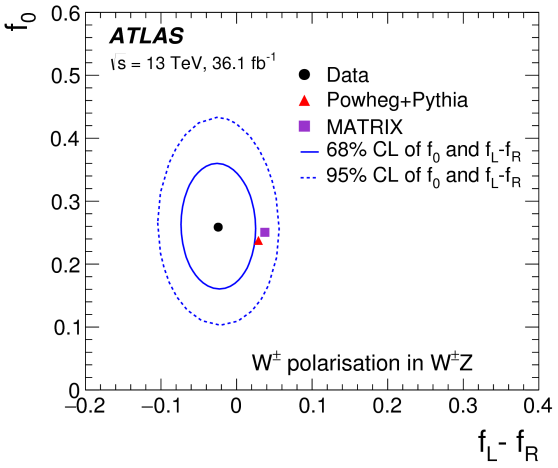

Figure 9: *WZ* measurement [2]. Measurement of the $W^\pm$ polarization in $W^\pm Z$ events, compared to the predictions from the SM. f_0, f_L, and f_R are the longitudinal, left and right-handed helicity fractions of $W^\pm$, respectively.

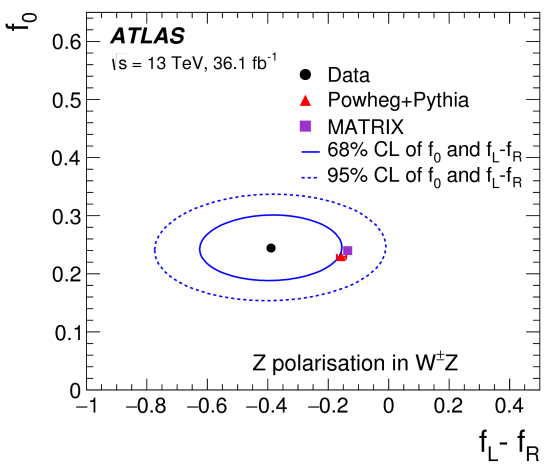

Figure 10: *WZ* measurement [2]. Measurement of the Z polarization in $W^\pm Z$ events, compared to the predictions from the SM. f_0, f_L, and f_R are the longitudinal, left and right-handed helicity fractions of Z, respectively.

7. Conclusion

The production cross sections of WW and WZ pairs have been measured at $\sqrt{s} = 13$ TeV using $36.1\,\text{fb}^{-1}$ of data recorded by the ATLAS detector at the LHC.

Unfolded differential production cross sections have been estimated for both WW and WZ productions, including observables sensitive to aTGC.

Competitive constraints have been derived on aTGC using the WW channel, in the framework of a dimension-6 Effective Field Theory. In addition, longitudinal and transverse helicity fractions of the W and Z bosons have been measured for the first time in diboson hadronic events via the WZ channel, and were found to be in agreement with the expectation from the SM.

References

[1] ATLAS Collaboration, *Measurement of differential W^+W^- production cross sections in proton-proton collisions at* 13 TeV *with the ATLAS detector*, CERN-EP-2019-055 [hep-ex/1905.04242].

[2] ATLAS Collaboration, *Precision WZ cross sections and polarisation at* 13 TeV, Eur. Phys. J. C 79 (2019) 535 [hep-ex/1902.05759].

[3] ATLAS Collaboration, *The ATLAS experiment at the CERN Large Hadron Collider*, J. Instrum. 3, (2008) S08003.

[4] ATLAS Collaboration, *Measurements of gluon-gluon fusion and vector-boson fusion Higgs boson production cross-sections in the $H \to WW^* \to e\nu\mu\nu$ decay channel in pp collisions at $\sqrt{s} = 13$ TeV with the ATLAS detector*, Phys. Lett. B 789 (2019) 508 [hep-ex/1808.09054].

[5] M. Grazzini *et al.*, *Fully differential NNLO computations with MATRIX*, Eur. Phys. J. C 78 (2018) 537 [hep-ph/1711.06631].

[6] E. Bothmann *et al.*, *Event Generation with Sherpa 2.2*, SciPost Phys. 7 (2019) 3 034 [hep-ph/1905.09127].

[7] G. D'Agostini, *Improved iterative Bayesian unfolding*, (2010) [physics.data-an/1010.0632].

[8] S. Alioli *et al.*, *A general framework for implementing NLO calculations in shower Monte Carlo programs: the POWHEG BOX*, J. High Energy Phys. 06 (2010) 043 [hep-ph/1002.2581].

[9] T. Sjöstrand *et al.*, *An introduction to PYTHIA 8.2*, Comput. Phys. Commun. 191 (2015) 159 [hep-ph/1410.3012].

[10] J. Bellm *et al.*, *Herwig 7.0/Herwig++ 3.0 release note*, Eur. Phys. J. C 76 (2016) 196 [hep-ph/1512.01178].

[11] C. Degrande *et al*, *Effective field theory: A modern approach to anomalous couplings*, Annals Phys. 335 (2013) 21 [hep-ph/1205.4231].

[12] J. Alwall *et al.*, *The automated computation of tree-level and next-to-leading order differential cross sections, and their matching to parton shower simulations*, J. High Energy Phys. 07 (2014) 079 [hep-ph/1405.0301].